

Infrared Laser Activation of Soluble and Membrane Protein Assemblies in the Gas Phase

Victor A. Mikhailov, Idlir Liko, Todd H. Mize, Matthew F. Bush,[†] Justin L. P. Benesch and Carol V. Robinson*

Department of Chemistry, Physical and Theoretical Chemistry Laboratory,
University of Oxford, Oxford, OX1 3QZ, United Kingdom

KEYWORDS *protein assemblies, membrane protein complexes, mass spectrometry, infrared multiphoton dissociation, IRMPD.*

ABSTRACT: Collision-induced dissociation (CID) is the dominant method for probing intact macromolecular complexes in the gas phase by means of mass spectrometry (MS). The energy obtained from collisional activation is dependent on the charge state of the ion, and the pressures and potentials within the instrument: these factors limit CID capability. Activation by infrared (IR) laser radiation offers an attractive alternative as the radiation energy absorbed by the ions is charge-state independent, and the intensity and timescale of activation is controlled by a laser source external to the mass spectrometer. Here we implement and apply IR activation, in different irradiation regimes, to study both soluble and membrane protein assemblies. We show that IR activation using high intensity pulsed lasers is faster than collisional and radiative cooling, and requires much lower energy than continuous IR irradiation. We demonstrate that IR activation is an effective means for studying membrane protein assemblies, and liberate an intact V-type ATPase complex from detergent micelles: a result that cannot be achieved by means of CID using standard collision energies. Notably, we find that IR activation can be sufficiently soft to retain specific lipids bound to the complex. We further demonstrate that, by applying a combination of collisional activation, mass selection, and IR activation of the liberated complex, we can elucidate subunit stoichiometry and the masses of specifically bound lipids in a single MS experiment.

INTRODUCTION

Mass spectrometry (MS) of intact protein assemblies from non-denaturing buffers is now a well-established approach in structural biology.¹⁻³ Recently this approach has been extended to membrane protein assemblies, using detergent micelles to maintain their solubility and preserve their interactions in the gas phase. Membrane protein complexes can then be liberated from gas-phase micelles. The most common MS means for activating protein assemblies is collision-induced dissociation (CID), achieved by collisions with neutral gas molecules or atoms.^{4,5} CID is used for soluble protein complexes to ‘clean’ them of residual buffer, and to promote dissociation of the non-covalent interactions within and between protein subunits, and ultimately to yield quaternary structural information.^{6,7} Collision activation is also used analogously for membrane protein complexes, to induce evaporation of the detergent molecules and thus free the complex from the encapsulating micelle,^{5,8} reveal its subunit composition,^{5,9-11} and to study lipid and drug binding.^{12,13}

Despite its widespread utility, CID has fundamental limits to its capability: the energy accumulated by the ion depends on its charge state, the accelerating potential applied to the collision cell, and the nature, number, and frequency of collisions.⁴ Numerous efforts have been made to overcome these

limitations. For example, it is possible to manipulate the energy by augmenting the charge of a gas-phase complex ion by adding “supercharging” reagents to the electrospray solution,^{14,15} employing different collision gases,¹⁶ or modifying the instrument to enable higher accelerating potentials,¹⁷ but these methods provide only limited benefit. Supercharging typically less than doubles the charge, and can lead to structural distortions in solution.¹⁸ Increasing the mass of the collision gas and its pressure increases the rate of internal energy deposition, but is met by diminishing returns, and can lead to ion losses *via* scattering and defocusing,⁴ whereas higher accelerating potentials require re-design of the hardware, and electronics within the mass spectrometer are limited to approximately a factor of two due to power supply and voltage breakdown difficulties.¹⁷ As a result, in >20 years since CID was first applied to protein assemblies,¹⁹ the advances have been incremental, and CID of many protein assemblies is not currently attainable.

The limitations of CID are magnified in the case of membrane protein complexes for which typically all available collisional activation has to be used to remove the micelle, rendering it impossible to fragment the detergent-free complex and elucidate its stoichiometry.¹¹ This means that the ideal of reverse-engineering protein complexes by CID, probing all

levels of structure through several steps of activation is a frontier challenge.^{17,20,21} As a result, there is an urgent need to develop orthogonal means for activating protein assemblies that are unencumbered by the limitations inherent to the mass spectrometer and charge on the ions.

Infrared multiphoton dissociation (IRMPD) employs IR lasers external to the mass spectrometer, and is an attractive alternative to CID as the amount of energy obtained by the ions during IR activation does not depend on their charge states and can be increased by raising the intensity of the radiation without compromising ion transfer and inducing ion losses.^{22,23} Like CID, IRMPD has been used in MS with great effect for sequencing of peptides and proteins.^{22,24-28} Commonly employed for this technique are continuous CO₂ lasers with 10.6 μm wavelength radiation. Both CID and continuous IRMPD (and its sister technique blackbody IR dissociation, BIRD)²⁹⁻³¹ are ‘slow heating’ methods that require hundreds of collisions or absorbed IR photons for the dissociation to occur.³² Usually, trapping the ions for long (≥ 10 ms) periods of irradiation is necessary to provide sufficient numbers of absorbed photons in IRMPD (Figure 1C).^{22,26,28,33} Elevated gas pressures are essential for relaxing initial kinetic energies of the ions of intact protein assemblies and storing them in electrodynamic traps,^{4,34} and therefore the energy-dissipating effect of collisional cooling is often unavoidable during their activation by continuous IR radiation, and results in a significant reduction of IRMPD efficiency.^{35,36}

Several faster activation techniques have been explored to dissociate gas-phase protein complexes on shorter time scales: UV photodissociation (UVPD),³⁷ electron capture or electron transfer dissociation (ECD / ETD),³⁸⁻⁴¹ and surface induced dissociation (SID).^{42,43} The latter is extremely efficient at generating structurally important fragments from protein complexes, but its off-axis geometry can lead to reduced ion transmission during the SID process due to scattering of the fragment ions produced by the impact on the surface. UVPD, ECD and ETD are efficient in cleaving the protein backbone, while the information obtained by these techniques on the non-covalent structure of protein assemblies is more limited (e.g., ECD and ETD produce fragments primarily from the unfolded regions of proteins). IRMPD can also be made much faster using pulsed IR lasers that provide high intensity output in the multi-kilowatt (kW) to megawatt (MW) range *versus* the 10-100 W power of continuous IR lasers. This leads to a significant reduction in activation time (from ≥ 10 ms to < 1 μs). Similar to the continuous IR activation, the pulsed regime is consistent with multiple photon absorption mechanism,⁴⁴ but the energy can be delivered to the gas-phase ions faster than the rate of deactivating collisions²⁸ or typical rates for radiative cooling (1-30 s^{-1}),^{36,45} avoiding interference from these two energy dissipating mechanisms. Although dissociation of the activated ions can take significantly longer times than the time of activation,⁴⁶ the dissociation rate constant increases rapidly with the energy of the activated ion,⁴⁷ and sub- μs dissociation times can be achieved with fast activation methods, as has been demonstrated for SID⁴⁸ and UV photodissociation^{49,50} of peptide ions.

In this work we implement continuous and pulsed IR laser radiation, in a Q-ToF mass spectrometer with minimal modifications, to investigate different regimes of IR activation

of the gas-phase protein assemblies. We demonstrate that both activation methods provide very efficient and controllable dissociation of soluble and membrane protein complexes. We show that IR laser irradiation is a ‘soft’ activation method: it can be used to liberate intact membrane protein complexes from micelles, and retain lipids specifically bound to the complex. Additionally, pulsed IR activation requires much less energy to achieve similar levels of dissociation efficiency than that provided by continuous IR activation, due to the faster activation of ions and the absence of deactivating cooling processes. Furthermore, pulsed IR activation can be used in sequence with other activation methods. We demonstrate this possibility through efficient IR dissociation of a membrane protein complex containing lipids after it has been liberated from the gas phase micelles by collisional activation. As a result, we propose that IRMPD is a flexible and versatile activation method with great potential for the study of protein assemblies.

EXPERIMENTAL SECTION

Materials and Proteins. Protein standards (avidin, glutamate hydrogenase, GroEL) and ammonium acetate were purchased from Sigma-Aldrich (St. Louis, MO). GroEL was further purified as described elsewhere.⁵¹ CS₂ hydrolase from *Acidianus A1-3* was a gift from Jasmin Mecinovic, Radboud University Nijmegen, Netherlands. V₀-V₁ ATPase from *Thermus thermophilus* was a gift from Daniela Stock, University of New South Wales, Sydney, Australia. P-glycoprotein (P-gp) was a gift from Geoffrey Chang, UC San Diego. Multi-antimicrobial extrusion membrane protein (MATE) fused with green fluorescent protein (GFP), ammonium channel (AmtB) and aquaporin-Z (AqpZ) were expressed and purified in-house as described elsewhere.⁵² Dodecyl maltoside (DDM), n-nonyl β -D-glucopyranoside (NG), octyltetraglycol (C8E4) and phosphatidylglycerol (PG) lipids were purchased from Avanti (Alabaster, AL).

Mass Spectrometry. IRMPD was implemented on an Ultima tandem quadrupole/time-of-flight (Q-ToF) mass spectrometer (Waters/Micromass, Manchester, UK). Initially the mass spectrometer was modified for high m/z transmission as described elsewhere.⁵³ CID experiments were carried out in the collision cell of the same mass spectrometer without ion trapping, or in a Q-ToF2 mass spectrometer (Waters/Micromass, Manchester, UK) modified to allow for the collision voltage of up to 400 V (200 V standard) as described elsewhere.¹¹ Protein solutions were nano-electrosprayed in 200 mM ammonium acetate, pH 7.5, at 1-5 μM concentrations with capillary voltage 1.4-1.7 kV and sampling cone voltage ranging from 100 V (avidin and CS₂ hydrolase) to 200 V (GroEL and membrane complexes). In the case of membrane proteins, detergent solution was prepared at twice the critical micelle concentration.

For the IRMPD experiments, the collision cell in the Ultima mass spectrometer was transformed into a linear ion trap by applying time-dependent controllable trapping voltages to its entrance and exit electrodes. The laser beam was steered into the mass spectrometer by gold-coated copper mirrors (Laser Beam Products, UK) and focused through the exit from the ion trap by a 50-cm focal length IR lens (ZnSe for 10.6 μm or

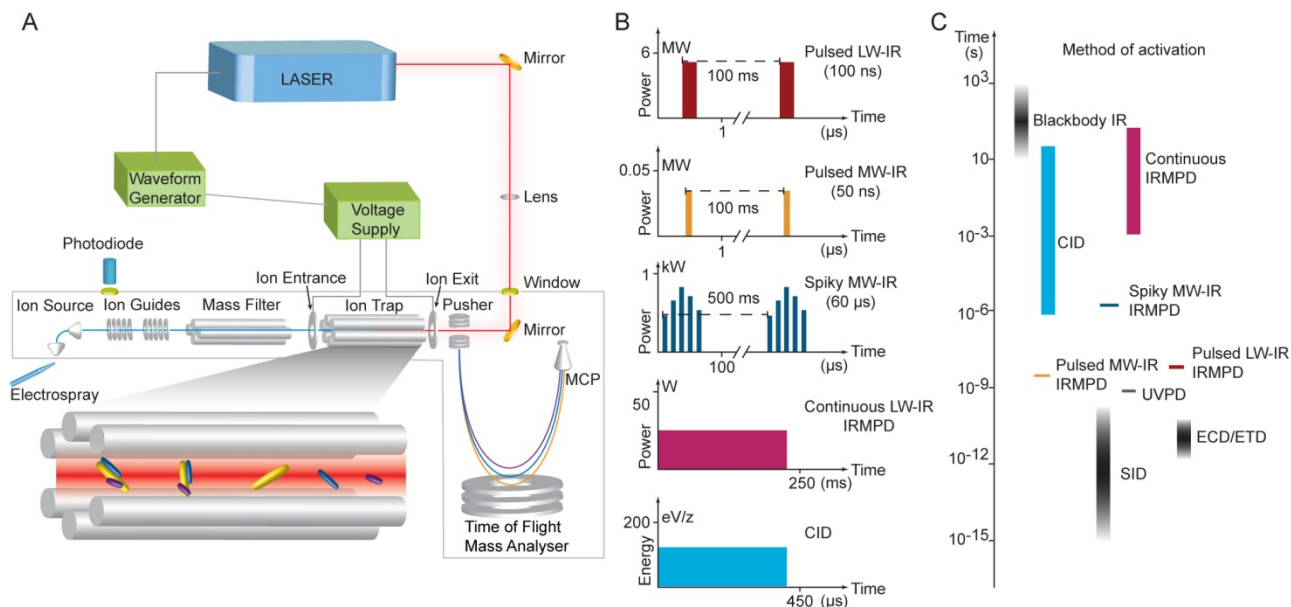


Figure 1. Experimental schematic and different regimes of ion activation. (A) Experimental setup: Protein complex ions formed by electrospray enter the mass spectrometer from the ion source region, pass through the ion guide and quadrupole mass filter, and are stored in the ion trap for laser dissociation. Fragment and precursor ions are mass analysed in the time-of-flight (ToF) detector, a multichannel plate (MCP) is used to convert ion current to electronic signal. The laser is either continuous or 100 ns pulsed LW-IR (10.6 μm wavelength), or pulsed MW-IR (single 50 ns or 60 μs ‘spiky’ pulses, 2.94 μm wavelength). (B) Regimes of ion activation used in this work: activation intensity versus time (see main text and Table S1 for details). (C) Comparison of the time scales of different gas-phase activation techniques³² used for the analysis of gas-phase protein assemblies.

CaF₂ for 2.94 μm , Crystran, UK).

An IR window and a gold-coated copper mirror were introduced in the ToF part of the instrument to steer the laser beam into the ion trap (Figure 1A). An IR photodiode (VIGO, Poland) was used to monitor the laser pulse quality and the alignment of the beam from the IR light scattered in the ion guide region (Figure 1A). Three IR lasers were used to provide IR radiation: a continuous CO₂ laser (48-2 Model, Synrad, Mukilteo, WA: 10.6 μm wavelength, 25 W), a pulsed CO₂ laser (Impact 4012, Lightmachinery, Canada: 10.6 μm , 0.58 J/pulse, 50-100 ns pulse duration), and a pulsed Er:YAG laser (Er:YAG 20-2, Spectrum, Germany: 2.94 μm wavelength). The Er:YAG laser is able to operate in two pulsed regimes: a ‘spiky’ long-pulse mode producing an array of low-intensity 500-ns laser pulses within a 60- μs envelope and with 40 mJ of total energy, or a short-pulse mode generating an intensive 50-ns pulse with 15 mJ energy (Figure 1B). During alignment, the laser power was also measured in the ion guide region, and scattering of the laser radiation due to the small apertures on the ion path were estimated. Laser beam parameters from manufacturers’ specifications were used to calculate beam area and radiation fluence along the axis of the ion trap for all three lasers (Figure S1 and Table S1, Supporting Information).

Four different activation regimes could be delivered using these three lasers: (i) continuous activation using long wavelength (LW) 10.6 μm IR radiation (commonly used in IRMPD), (ii) single-pulse 10.6 μm LW-IR activation, and (iii) two single-pulse regimes (50 ns or 60 μs) provided by the 2.94 μm IR laser (medium wavelength, MW-IR activation). The continuous LW-IR regime was characterized by a low-intensity

(< 25 W) and long activation time (100-250 ms) whereas the LW and MW-IR pulsed regimes provided a short-time (50 -100 ns) and high-intensity (0.3-5.5 MW) activation (Figure 1B, C). The average pulse intensity (~700 W) and duration (60 μs) of the ‘spiky’ MW-IR radiation were intermediate to the continuous and 50-100 ns pulsed regimes (Figure 1B). Changing the energy of IR activation was achieved by changing the output power of the lasers when required. The trapping time was kept constant during energy-dependent measurements.

Operation of the trap was synchronized with operation of the lasers using a waveform generator (Agilent, Santa Clara, CA). When the continuous laser was used, the trap was open for the protein ions to enter during the complete irradiation time (*ca.* 100-250 ms) in order to maximize the number of electrosprayed complexes subjected to activation. At the end of trapping/irradiation period, voltages at the entrance and exit electrodes of the collision cell were changed for a period of 7 ms to the values that allowed ejection of the ions into the ToF analyzer. For pulsed laser activation, the ions were stored in the trap for a period of *ca.* 100-500 ms. At the end of this period, a laser pulse was fired followed by ejection of the ions into the ToF analyzer and their detection by a multichannel plate (MCP). IRMPD mass spectra presented here are produced by averaging over a period of 10-100 s.

RESULTS AND DISCUSSION

Pulsed IRMPD requires lower energy than continuous LW irradiation. First we investigated dissociation of soluble protein complexes under different regimes of IR activation. For

avidin, a 64 kDa tetramer (Figure S2A), IRMPD with the continuous LW-IR laser resulted in depletion of the tetramer ions and production of monomer and trimer fragment ions with the initial charge of the complex divided approximately equally between the monomers and trimers (Figure 2A, top). These fragments are consistent with charge-asymmetric dissociation that results in unfolded and highly charged monomeric subunits and charge-stripped oligomeric fragments, as observed previously with continuous IMRPD.⁵⁴ Asymmetric dissociation is also commonly observed following CID.⁶ For comparison, CID of avidin with 150 V collision voltage produced similar fragments with efficiency comparable to continuous IRMPD (Figure S2).

To investigate the effect of accelerating IRMPD, we switched to the high power / short radiation time regime of pulsed IR activation of our 100-ns pulsed LW-IR laser. This also resulted in asymmetric dissociation (Figure 2A), but the pulsed IR activation regime produced a significant amount of fragment ions at much lower activation energies. The maximum laser pulse energy from the pulsed laser (~0.5 J) was over an order of magnitude smaller than the maximum energy of 5.6 J (maximum laser power \times irradiation time) provided by the continuous IR laser, yet provided comparable fragmentation yields. We also observed a similar effect for the pulsed 2.94 μ m MW-IR activation of avidin, recording significant amounts of dissociation of avidin at the markedly lower energies of 40 and 15 mJ, for 60- μ s ‘spiky’ pulses and 50-ns pulses, respectively (Figure S2C, D). These results demonstrate how increasing the speed of energy deposition can dramatically reduce the requirement for laser power.

To ascertain whether the source of this improvement lies in the faster dynamics of pulsed IR activation tipping the balance between activation and deactivation of the trapped ions, we measured the dissociation efficiency in both activation methods as a function of the number of cooling collisions experienced by the ions in the trap. The number of collisions was varied by increasing the pressure of the bath gas (Ar) in the ion trap while keeping the laser energy and trapping time constant. In the case of continuous IRMPD, increasing the pressure by one order of magnitude (from *ca.* 10^{-4} to 10^{-3} mbar) caused a decrease in the product yield from ~90% to 6% (Figure S3A). A similar change in the trapping pressure did not affect the efficiency of pulsed IRMPD (Figure S3B).

These measurements can be rationalised by estimating the frequency of cooling collisions in the ion trap. For the trapping pressure of 10^{-4} mbar of argon the characteristic time between the collisions is approximately 16 μ s, Note S1 (Supporting Information). Therefore, a large number of cooling collisions take place during the *ca.* 250 ms time of activation by the continuous laser. These collisions reduce the efficiency of activation of the avidin complexes by dissipating the energy absorbed from the IR radiation, with the deactivating effect increasing with the gas pressure (Figure S3).

In contrast to continuous activation, the 50-100-ns activation times delivered by the pulsed MW and LW-IR lasers are much smaller than the average time between the collisions, and no significant dissipation of internal energy through collisions takes place during the activation. Furthermore, the rate of the 100-ns pulsed IR activation is also much faster than the characteristic rates for radiative cooling of gas-phase polyatomic ions ($\sim 1 - 30 \text{ s}^{-1}$),^{36,45} thus this dissipation mechanism is effectively ‘switched off’. In the ‘middle time/

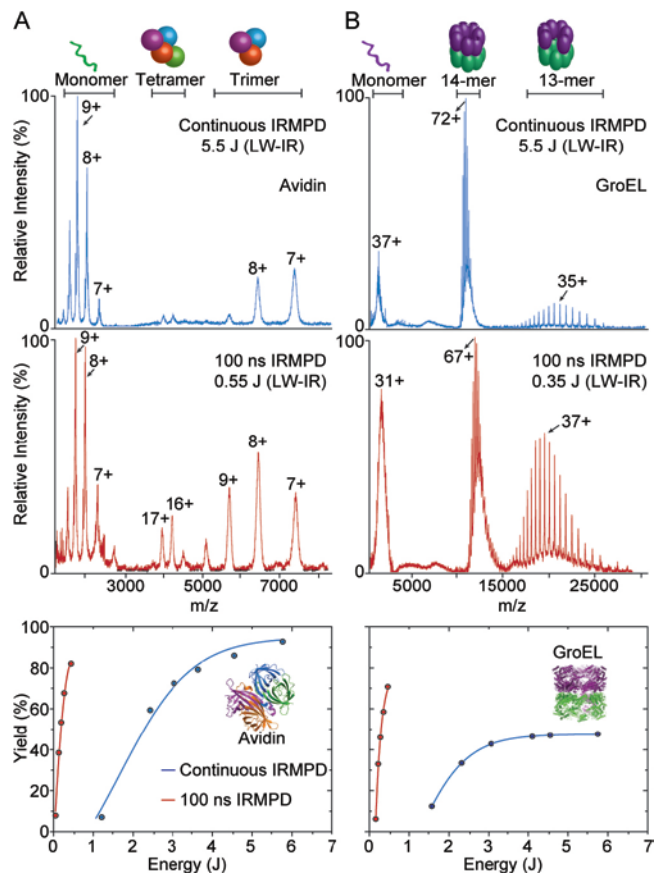


Figure 2. Gas phase dissociation of soluble protein complexes under different regimes of activation. (A) avidin tetramer ions (64 kDa) in charge states from 15+ to 17+ undergo asymmetric dissociation via the loss of an unfolded monomeric subunit. (B) GroEL tetradecamer ions (803 kDa) in charge states from 60+ to 75+ dissociate into unfolded subunits and tridecamers, most abundant charge states of the 14-mer precursor ions, monomer and the 13-mer fragment ions are indicated. Graphs – product yield from IRMPD for pulsed and continuous activation (trapping time = 243 ms) versus IR energy delivered into the ion trap. Yield measurements for each energy value were done in triplicates with standard deviation varied between 3 and 6 %.

middle energy’ case of 60 μ s ‘spiky’ MW-IR activation there are very few cooling collisions taking place during the 60 μ s activation in comparison with the continuous regime (~250 ms), thus IRMPD can take place at low, 40 mJ pulse energy (Figure S2C). Additionally, in both cases of 50 ns and 60 μ s MW-IR irradiation, the energy obtained from the absorption of a single photon is 3.6 times higher than in the case of LW-IR activation, thus the number of absorption events needed to reach the barrier to dissociation is proportionally smaller, so the dissociation becomes possible even at lower (15-40 mJ) IR pulse energy (Figure S2C, D).

Higher bath gas pressures are required for transmission and trapping of heavier complexes,^{4,55} and collisional cross sections of protein complexes increase with the mass of the complex.¹⁸ In order to test whether pulsed IR activation could also be advantageous for larger protein complexes we carried out IRMPD of the GroEL tetradecamer (803 kDa) in both activation regimes. Pulsed 100-ns LW-IR activation produced a larger quantity of fragments from GroEL than continuous LW-IR activation (~77 % versus 52% at maximum energy) while requiring a much smaller energy (Figure 2B). This result is in

accord with our estimation for the rate of cooling collisions for the trapped GroEL ions. The collision cross section of GroEL ions ($219\text{--}244\text{ nm}^2$)^{56,57} is greater than that of avidin ions (*ca.* 42 nm^2),⁵⁶ and higher trapping pressures ($\geq 10^{-3}$ mbar) are required for the larger GroEL ions. Both these factors could conspire to produce significant deactivation of GroEL during continuous IR activation. Although the average time between cooling collisions for GroEL was much shorter than the one for avidin, *ca.* $0.28\text{ }\mu\text{s}$ (Note S1), it still remains significantly longer than the 100-ns LW-IR pulse duration. As a result, pulsed IR activation results in extremely efficient dissociation.

Symmetric dissociation is possible under pulsed IRMPD.

In the examples above, pulsed IR activation of protein complexes resulted in asymmetric dissociation, in which the mass-charge-density of the product ions is very different. This is the most common dissociation route of protein complexes under CID, and also previously reported for continuous IRMPD.^{54,58} Symmetric dissociation of protein complexes have been achieved by SID^{42,43} and, in some cases, by CID.^{18,59} In symmetric dissociation, the charges taken by sub-oligomer fragments from the precursor complex are proportional to the number of subunits in the fragment. These fragments have compact structures close to the native ones, as shown by measurements of their collisional cross sections,^{18,42} and are thus valuable for understanding the structure of the complex. Symmetric dissociation is thought to take place when the activation and dissociation of the complex happens faster than the time necessary for protein unfolding.^{42,43}

It was shown that charge-reduced ions produce symmetric and compact fragments under SID.⁴¹ We have investigated pulsed IRMPD of charge-reduced ions of several protein complexes. Our data on charged reduced ions of avidin and CS₂ hydrolase octamer (189 kDa)⁶⁰ are included in Figures S2 and S4. The dissociation proceeded along the asymmetrical pathway (loss of an unfolded subunit), albeit the charge states of the fragments are lower than from ‘normally’ charged ions, which implies that the fragments may be more compact.

Previously we reported symmetric dissociation from CID of supercharged SAP pentamer.¹⁸ ‘Supercharging’ of electrosprayed proteins can be achieved through additives, *e.g.* sulfolane, to the electrospray solution. Here we investigated pulsed 100-ns LW-IR activation to dissociate supercharged ions of the CS₂ hydrolase octamer. Unlike the asymmetric dissociation of the lower charge states (Figure S4), both asymmetric (monomers and heptamers) and symmetric (dimers and tetramers) dissociation of the higher charge states was observed (*e.g.* 36+ state, Figure 3). The dimers in the CS₂ hydrolase complex are structurally important, because they form the ‘corners’ of the square ring of the octamer’s structure (Figure 3A, inset). Similar results were obtained with CID, albeit with a lower yield of symmetric products from the supercharged complexes (12% *vs* 37% from IRMPD at maximum activation energy, Figure 3C, D). The higher yield of the fragments from symmetric dissociation in the case of pulsed IRMPD is likely to be related to the more instantaneous nature of pulsed IR activation, with a higher proportion of the complexes dissociating before subunit unfolding could take place along the asymmetric dissociation pathway.^{61,62}

We also observed symmetric dissociation of the glutamate dehydrogenase (GD) dodecamer under pulsed IRMPD. GD dodecamer is a non-specific dimer of the GD hexamer complex (337 kDa). In contrast to other nonspecific adducts of protein complexes, *e.g.* avidin octamer (Figure S2B) or GroEL 28-

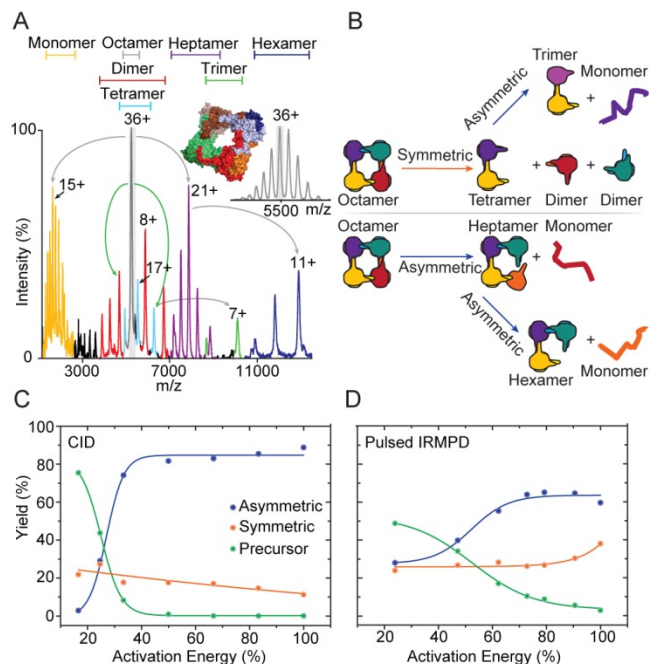


Figure 3. Example of symmetric dissociation under pulsed IRMPD. (A) 100 ns LW-IR activation of the ‘supercharged’ 36+ ions of CS₂ hydrolase. Inset left: the crystal structure of the hydrolase octamer (3TEN in PDB). Inset right: charge states of the ‘supercharged’ octamer. Pulsed IRMPD results in both asymmetric (monomers, heptamers and hexamers) and symmetric (dimers and tetramers) dissociation. Trimers are produced by further asymmetric dissociation of the tetramers. (B) Diagram of the symmetric and asymmetric pathways for the dissociation of the hydrolase octamer. (C) and (D) Abundance of the precursor octamer ions, symmetric and asymmetric fragments from CID and 100 ns IRMPD, respectively, versus activation energy (0.55 J = 100 % for IRMPD, 150 V = 100 % for CID. Standard deviation for yield values as in Figure 2.

mer,⁵⁴ GD dodecamer dissociates symmetrically into the constituent hexamers under both IRMPD and CID,⁶³ whilst the asymmetric dissociation of hexamers is hindered (Figure S5).

Our results for avidin, GroEL, CS₂ hydrolase and other soluble complexes (data not presented here) demonstrate that although pulsed 50-100-ns IRMPD takes place on the time scale faster than the cooling processes, asymmetric dissociation remains the dominant channel in most cases (*e.g.*, Figures 2, 3 and Figures S2, S4). CID and continuous IRMPD are ‘slow-heating’ processes that happen on the time scale longer than intramolecular vibrational redistribution (IVR) of internal energy in the activated ion, in condition of quasi-equilibrium of the internal energy and *via* statistically favourable dissociation pathways with the lowest activation energies.^{64,65} Both activations usually result in the asymmetric dissociation in the case of non-covalent protein.^{4,54} IVR during IR activation used in this work redistributes the energy absorbed by the C-O vibrations (LW-IR, $10.6\text{ }\mu\text{m}$) or O-H vibrations (MW-IR, $2.94\text{ }\mu\text{m}$) among all other vibrations in the protein complex until the complex accumulates sufficient internal energy to dissociate.

Characteristic IVR times have been measured for proteins in solution and demonstrated to be in the picosecond range,⁶⁶⁻⁶⁸ but, to our knowledge, no gas-phase measurements for intact protein assemblies exist in the literature. Based on our results, we conclude that IVR in protein assemblies happens on a time

scale of $\ll 50$ ns and defines the observed fragmentation patterns. Generation of the symmetric fragments on a larger time scale used here requires either a change in the balance of electrostatic repulsion between the subunits and non-covalent binding (e.g. supercharging of CS₂ hydrolase complexes), or presence of a barrier to the protein unfolding upon activation (e.g. GD dodecamer).

IR activation liberates intact membrane protein complexes. Electrospray MS of membrane proteins or their complexes in detergent micelles results in a broad featureless ion signal, and collisional activation is usually employed to evaporate the detergent and resolve the charge states of the protein ions.⁸ In some cases, as we show below, higher than typical levels of collisional activation are required, and this can only be achieved by considerable modification of the mass spectrometer.

We have explored pulsed and continuous IR radiation as an alternative means of releasing membrane protein complexes from gas-phase micelles for MS analysis. We stored electrosprayed complexes in micelles in the ion trap and subjected them to IR activation. The range of the membrane proteins that we investigated spanned from monomeric proteins MATE-GFP, 78 kDa, and P-gp, 142 kDa, (Figure S6A-D), through trimeric AmtB, 127 kDa, (Figure S6E-H) and AqpZ tetramer, 99 kDa, (Figure 4), to a large multiprotein assembly of the V-type ATPase, 690 kDa (Figure 4). Both pulsed and continuous 10.6 μ m LW-IR radiation could effectively evaporate detergent molecules from a membrane protein or a protein complex, and its charge states could then be resolved (Figures 4 and S6). Furthermore, releasing membrane protein complexes from micelles by LW-IR radiation was possible for a range of micelle-forming detergents (e.g. DDM, NG and C8E4). Pulsed 2.94 μ m MW-IR activation was also able to release membrane proteins from gas-phase micelles, but the efficiency was lower, with part of the broad ion signal from the proteins in micelles was still observed (Figure S6). This could be due to the much lower pulse energy of MW-IR radiation (40 mJ *versus* 550 mJ in LW-IR), and also indicative of the slow-heating nature of detergent evaporation by IR radiation.

We also found that mass selection of ions from a part of the broad ion signal from proteins in micelles using the quadrupole mass filter before the IR activation (Figure 1) could improve the mass spectra by reducing the amount of chemical noise from the detergent (Figure S6E-G). Furthermore, mass selection can also be used to manipulate the charge-state distribution of the released protein complex and the degree of its fragmentation (Figure 4A).

We used a combination of mass selection and IR activation to obtain mass spectra of intact V-type ATPase from *Thermus thermophilus* (690 kDa). This large multi-subunit assembly is a complicated molecular machine that represents a challenging target for native MS analysis.^{10,69} Importantly, the standard range of collisional energy (accelerating voltage ≤ 200 V) available in the collision cell of the mass spectrometer was not sufficient for releasing this protein assembly intact from DDM micelles with resolution of its charge states (Figure 4A, top right). By contrast we were able to liberate ATPase from DDM micelles using a standard continuous LW-IR laser. First, we selected, trapped and activated ions from within the broad range of signal from the ATPase in DDM micelles. This resulted in the liberation of the intact ATPase in relatively low charge states centred at $z = 37+$, and no noticeable dissociation was recorded (Figure 4A, left). Mass-selection of the ions from a

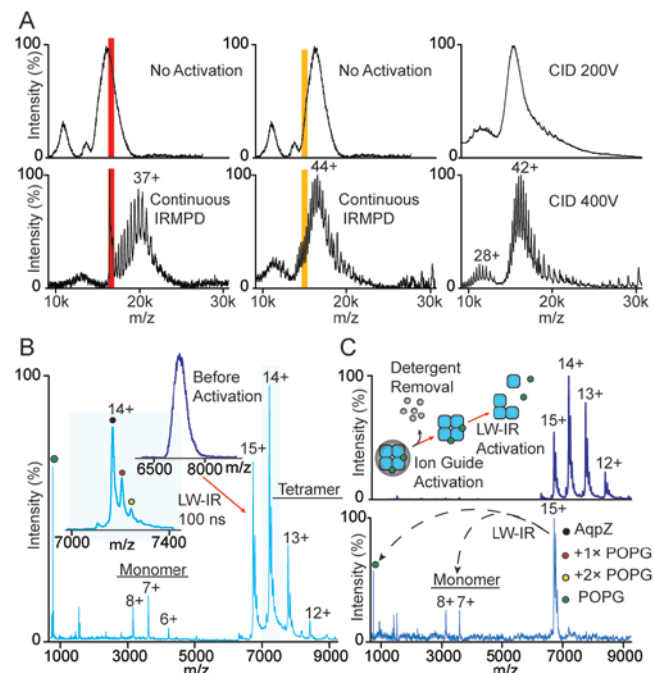


Figure 4. Mass spectra of membrane proteins. (A) V₀-V₁ ATPase (690 kDa) in DDM micelles: before and after LW-IR (10.6 μ m) activation of the ions from the descending (left) and ascending (centre) parts of the signal from the complexes in micelles, and after 200 V and 400 V collisional activation (top and bottom right, respectively). (B) Aquaporin-Z (AqpZ) tetramer with bound PG lipids released from C₈E₄ micelles by 100-ns LW-IR activation. Inset: zoom-in of the 15⁺ charge state of the liberated complex showing the presence of the apo-tetramer and the tetramers with PG lipids attached. (C) Charge states of AqpZ released from detergent micelles by collisional activation in the ion guide (top), and the 100-ns LW-IRMPD of the mass selected 15⁺ charge state of the released AqpZ tetramer yielding dissociated lipids and unfolded protein monomers (bottom).

different region of the signal followed by IR activation resulted in higher charge states of the intact ATPase around $z = 45+$, and some dissociation of subunits was observed (recorded at $m/z > 25,000$) (Figure 4A, centre). With collision voltage of 400V, using a mass spectrometer modified for elevated collisional energies, we could resolve charge states from the same sample used in our IRMPD studies (Figure 4A, bottom right). This emphasises how IR laser activation can efficiently liberate membrane protein complexes from the gas-phase micelles.

We also note that, in all cases of LW-IR and MW-IR activation, when a membrane protein complex underwent some dissociation, after being liberated from the micelle, the dissociation followed the asymmetric pathway, similar to soluble complexes and was therefore determined by the IVR mechanism (Figure 4B and Figure S6).

IR activation allows the elucidation of protein-lipid interactions. Next we investigated the action of IR activation on the membrane protein complexes with bound lipids. Lipids play crucial roles in complex structure and function,⁷⁰ and therefore it is important to reveal the nature of the lipids bound to the complex. Previously we demonstrated that using controllable collisional activation it is possible to liberate an intact membrane complex from detergent micelles and retain lipids bound to the intact complex.^{12,13} One might expect that in the case of IR activation, which was absorbed by lipids as well

as by micelles, the lipids could be lost when the complex was released from the micelles. Contrary to this expectation, our results for aquaporin-Z tetramer with PG lipids demonstrate that IR activation is sufficiently gentle, and the tetramer-lipid complexes were preserved in mass spectra (Figure 4B).

IR activation of the ions from the broad ion signal assigned to AqpZ in detergent micelles also produced some low-mass ions: protein monomers and PG lipids (Figure 4B), which presumably originated from the partial dissociation of the protein/lipid complex. The lipid mass can be elucidated from the mass spectral peaks produced by singly-charged lipids with higher accuracy than from the mass peaks produced by multiply-charged complexes with bound lipids. However, some of the free lipids observed in Figure 4B could be the ones contained in the micelles in non-bound form and then released by IR activation. In order to identify the lipids that are actually bound to the complex it is necessary first to isolate complexes from the gas-phase micelles, and then fragment the detergent-free complexes, releasing lipids for mass analysis. We achieved the first step in this approach by promoting collisional activation of the complexes in micelles in the ion guide of the mass spectrometer by raising the accelerating potential between the two parts of the ion guide to maximum (Figure 1). As the residual pressure was relatively high in the ion guide region, *ca.* 3-10 mbar, intensive collisions with the molecules of atmospheric gases could thus be induced. After aquaporin-Z tetramer in C8E4 micelles was released from the detergent micelles in the ion guide, the 15+ charge state containing both unbound and bound PG lipids, was mass selected and dissociated by using pulsed IRMPD, releasing monomeric subunits and component lipids from the complex (Figure 4C). As a result, employing this multi-stage fragmentation approach allows both complex stoichiometry and the mass of the bound lipid to be elucidated in a single MS experiment.

CONCLUSIONS

We have demonstrated that gas-phase IR laser activation is an efficient and sensitive method for MS analysis of both soluble and membrane protein assemblies. We have recapitulated all essential results achieved by collisional activation over the previous period of development of the non-denaturing MS approach. Furthermore, IR activation method has a flexibility of switching between different regimes of irradiation, such as pulsed or continuous in the LW or MW IR spectral range. Activation by pulsed IR lasers provides an advantage by operating faster than cooling deactivation of the irradiated ions and thus less energy is required for dissociation. IR radiation can also be used as a 'soft' method of activation to release membrane complexes, intact or with low degree of dissociation, from a variety of detergent micelles used for solubilisation and electrospray ionization.

Importantly, for structural and functional studies of membrane proteins, IR activation is sufficiently gentle to retain specific lipids attached to the complex liberated from the micelle. We have also shown that probing a mass-selected charge state of a detergent-stripped membrane protein complex by IR multiphoton dissociation can be carried out after the detergent molecules are removed by collisional activation: this approach paves the way for studying specific lipid binding to membrane proteins. IRMPD of detergent-free membrane protein complexes and soluble protein complexes usually follows the pathway previously described for CID (asymmetric dissociation) for the times of IR activation ≥ 50 ns. Alternative

(symmetric) dissociation results in more structural information, and can be achieved for some protein complexes by IR activation of their supercharged ions. Our results demonstrate that laser photoactivation is a versatile technique: its further progress in application to gas-phase protein assemblies should readily follow the employment of lasers generating even shorter and more intensive radiation pulses in order to produce more structurally important fragments for a larger range of protein complexes.

ASSOCIATED CONTENT

Supporting Information. The contents of Supporting Information include a table of parameters of IR irradiation regimes, a note on estimation of the rate of cooling collisions, dissociation MS/MS spectra (CID, IRMPD) of avidin tetramer and octamer at different conditions, CID MS/MS spectra of CS₂ hydrolase octamer, IRMPD MS/MS spectra of glutamate dehydrogenase hexamer and dodecamer, and mass spectra of several membrane proteins after IR activation. This material is available free of charge via the Internet at <http://pubs.acs.org>.

AUTHOR INFORMATION

Corresponding Author

* carol.robinson@chem.ox.ac.uk

Present Addresses

[†] Department of Chemistry, University of Washington, Box 351700, Seattle, WA 98195-1700

The authors declare no competing financial interest.

ACKNOWLEDGMENT

We thank the Medical Research Council UK (G1000819), the ERC (IMPRESS) for financial support (ERC 268851), the CLF, UK for the gift of a laser from the retiring loan pool, and Waters Corporation for an Industrial Fellowship for VAM. We gratefully acknowledge Jasmin Mecinovic from Radboud University Nijmegen, Netherlands for the sample of CS₂ hydrolase, Daniela Stock from University of New South Wales, Sydney for V-type ATPase. Tony Gilbert, Jeff Brown, Steven Pringle and Darren Hewitt from Waters Corporation, and Ken Ure from Lightmachinery for technical support and helpful discussions. Rainer Cramer from the University of Reading for lending an Er:YAG laser.

REFERENCES

- (1) Hilton, G. R.; Benesch, J. L. P. *J. R. Soc., Interface* **2012**, *9*, 801-816.
- (2) Marcoux, J.; Robinson, C. V. *Structure (London, England : 1993)* **2013**, *21*, 1541-1550.
- (3) Sharon, M. *Science* **2013**, *340*, 1059-1060.
- (4) Benesch, J. L. P.; Ruotolo, B. T.; Simmons, D. A.; Robinson, C. V. *Chem. Rev.* **2007**, *107*, 3544-3567.
- (5) Laganowsky, A.; Reading, E.; Hopper, J. T. S.; Robinson, C. V. *Nat. Protoc.* **2013**, *8*, 639-651.
- (6) Benesch, J. L. P. *J. Am. Soc. Mass Spectrom.* **2009**, *20*, 341-348.
- (7) Hall, Z.; Politis, A.; Robinson, C. V. *Structure* **2012**, *20*, 1596-1609.
- (8) Barrera, N. P.; Di Bartolo, N.; Booth, P. J.; Robinson, C. V. *Science* **2008**, *321*, 243-246.
- (9) Barrera, N. P.; Robinson, C. V. In *Annual Review of Biochemistry*, Vol 80, Kornberg, R. D.; Raetz, C. R. H.; Rothman, J. E.; Thorner, J. W., Eds., 2011, pp 247-271.
- (10) Zhou, M.; Morgner, N.; Barrera, N. P.; Politis, A.; Isaacson, S. C.; Matak-Vinkovic, D.; Murata, T.; Bernal, R. A.; Stock, D.; Robinson, C. V. *Science* **2011**, *334*, 380-385.

- (11) Hopper, J. T. S.; Yu, Y. T.-C.; Li, D.; Raymond, A.; Bostock, M.; Liko, I.; Mikhailov, V.; Laganowsky, A.; Benesch, J. L. P.; Caffrey, M.; Nietlispach, D.; Robinson, C. V. *Nat. Methods* **2013**, *10*, 1206-+.
- (12) Marcoux, J.; Wang, S. C.; Politis, A.; Reading, E.; Ma, J.; Biggin, P. C.; Zhou, M.; Tao, H.; Zhang, Q.; Chang, G.; Morgner, N.; Robinson, C. V. *PNAS USA* **2013**, *110*, 9704-9709.
- (13) Laganowsky, A.; Reading, E.; Allison, T. M.; Ulmschneider, M. B.; Degiacomi, M. T.; Baldwin, A. J.; Robinson, C. V. *Nature* **2014**, *510*, 172-+.
- (14) Iavarone, A. T.; Williams, E. R. *J. Am. Chem. Soc.* **2003**, *125*, 2319-2327.
- (15) Sterling, H. J.; Kintzer, A. F.; Feld, G. K.; Cassou, C. A.; Krantz, B. A.; Williams, E. R. *J. Am. Soc. Mass Spectrom.* **2012**, *23*, 191-200.
- (16) Lorenzen, K.; Versluis, C.; van Duijn, E.; van den Heuvel, R. H. H.; Heck, A. J. R. *Int. J. Mass spectrom.* **2007**, *268*, 198-206.
- (17) Benesch, J. L. P.; Ruotolo, B. T.; Sobott, F.; Wildgoose, J.; Gilbert, A.; Bateman, R.; Robinson, C. V. *Anal. Chem.* **2009**, *81*, 1270-1274.
- (18) Hall, Z.; Politis, A.; Bush, M. F.; Smith, L. J.; Robinson, C. V. *J. Am. Chem. Soc.* **2012**, *134*, 3429-3438.
- (19) Lightwahl, K. J.; Winger, B. E.; Smith, R. D. *J. Am. Chem. Soc.* **1993**, *115*, 5869-5870.
- (20) Belov, M. E.; Damoc, E.; Denisov, E.; Compton, P. D.; Horning, S.; Makarov, A. A.; Kelleher, N. L. *Anal. Chem.* **2013**, *85*, 11163-11173.
- (21) Rathore, D.; Aboufazeli, F.; Dodds, E. D. *Analyst* **2015**, *140*, 7175-7183.
- (22) Brodbelt, J. S.; Wilson, J. J. *Mass Spectrom. Rev.* **2009**, *28*, 390-424.
- (23) Raspopov, S. A.; El-Faramawy, A.; Thomson, B. A.; Siu, K. W. M. *Anal. Chem.* **2006**, *78*, 4572-4577.
- (24) Little, D. P.; Speir, J. P.; Senko, M. W.; Oconnor, P. B.; McLafferty, F. W. *Anal. Chem.* **1994**, *66*, 2809-2815.
- (25) Fridriksson, E. K.; Baird, B.; McLafferty, F. W. *J. Am. Soc. Mass Spectrom.* **1999**, *10*, 453-455.
- (26) Oh, H.; Breuker, K.; Sze, S. K.; Ge, Y.; Carpenter, B. K.; McLafferty, F. W. *PNAS USA* **2002**, *99*, 15863-15868.
- (27) Wigger, M.; Eyler, J. R.; Benner, S. A.; Li, W. Q.; Marshall, A. G. *J. Am. Soc. Mass Spectrom.* **2002**, *13*, 1162-1169.
- (28) Gabrylski, W.; Li, L. *Rapid Commun. Mass Spectrom.* **2002**, *16*, 1805-1811.
- (29) Ying, G.; Horn, D. A.; McLafferty, F. W. *Int. J. Mass spectrom.* **2001**, *210-211*, 203-214.
- (30) Jockusch, R. A.; Schnier, P. D.; Price, W. D.; Strittmatter, E. F.; Demirev, P. A.; Williams, E. R. *Anal. Chem.* **1997**, *69*, 1119-1126.
- (31) Klassen, J. S.; Weijie, W.; Kitova, E. N.; Jiangxiao, S. *J. Am. Soc. Mass Spectrom.* **2005**, *16*, 1583-1594.
- (32) McLuckey, S. A.; Goeringer, D. E. *J. Mass Spectrom.* **1997**, *32*, 461-474.
- (33) Gardner, M. W.; Smith, S. I.; Ledvina, A. R.; Madsen, J. A.; Coon, J. J.; Schwartz, J. C.; Stafford, G. C., Jr.; Brodbelt, J. S. *Anal. Chem.* **2009**, *81*, 8109-8118.
- (34) Heck, A. J. R. *Nat. Methods* **2008**, *5*, 927-933.
- (35) Madsen, J. A.; Gardner, M. W.; Smith, S. I.; Ledvina, A. R.; Coon, J. J.; Schwartz, J. C.; Stafford, G. C., Jr.; Brodbelt, J. S. *Anal. Chem.* **2009**, *81*, 8677-8686.
- (36) Glish, G. L.; Black, D. M.; Payne, A. H. *J. Am. Soc. Mass Spectrom.* **2006**, *17*, 932-938.
- (37) O'Brien, J. P.; Li, W.; Zhang, Y.; Brodbelt, J. S. *J. Am. Chem. Soc.* **2014**, *136*, 12920-12928.
- (38) Geels, R. B. J.; van der Vies, S. M.; Heck, A. J. R.; Heeren, R. M. A. *Anal. Chem.* **2006**, *78*, 7191-7196.
- (39) Zhang, H.; Cui, W.; Wen, J.; Blankenship, R. E.; Gross, M. L. *J. Am. Soc. Mass Spectrom.* **2010**, *21*, 1966-1968.
- (40) Zhang, H.; Cui, W.; Wen, J.; Blankenship, R. E.; Gross, M. L. *Anal. Chem.* **2011**, *83*, 5598-5606.
- (41) Lermyte, F.; Konijnenberg, A.; Williams, J. P.; Brown, J. M.; Valkenborg, D.; Sobott, F. *J. Am. Soc. Mass Spectrom.* **2014**, *25*, 343-350.
- (42) Mowei, Z.; Shai, D.; Wysocki, V. H. *Angew. Chem. Int. Ed.* **2012**, *51*, 4336-4339.
- (43) Zhou, M.; Jones, C. M.; Wysocki, V. H. *Anal. Chem.* **2013**, *85*, 8262-8267.
- (44) von Helden, G.; Oomens, J.; Sartakov, B. G.; Meijer, G. *Int. J. Mass spectrom.* **2006**, *254*, 1-19.
- (45) Dunbar, R. C. *Mass Spectrom. Rev.* **1992**, *11*, 309-339.
- (46) Laskin, J.; Bailey, T. H.; Futrell, J. H. *Int. J. Mass spectrom.* **2004**, *234*, 89-99.
- (47) Baer, T.; Mayer, P. M. *J. Am. Soc. Mass Spectrom.* **1997**, *8*, 103-115.
- (48) Gamage, C. M.; Fernandez, F. M.; Kuppannan, K.; Wysocki, V. H. *Anal. Chem.* **2004**, *76*, 5080-5091.
- (49) Yoon, S. H.; Kim, M. S. *J. Am. Soc. Mass Spectrom.* **2007**, *18*, 1729-1739.
- (50) Moon, J. H.; Yoon, S.; Bae, Y. J.; Kim, M. S. *Mass Spectrom. Rev.* **2015**, *34*, 94-115.
- (51) Hernandez, H.; Robinson, C. V. *Nat. Protoc.* **2007**, *2*, 715-726.
- (52) Reading, E.; Liko, I.; Allison, T. M.; Benesch, J. L. P.; Laganowsky, A.; Robinson, C. V. *Angewandte Chemie-International Edition* **2015**, *54*, 4577-4581.
- (53) Sobott, F.; Hernandez, H.; McCammon, M. G.; Tito, M. A.; Robinson, C. V. *Anal. Chem.* **2002**, *74*, 1402-1407.
- (54) El-Faramawy, A.; Guo, Y.; Verkerk, U. H.; Thomson, B. A.; Siu, K. W. M. *Anal. Chem.* **2010**, *82*, 9878-9884.
- (55) Chernushevich, I. V.; Thomson, B. A. *Anal. Chem.* **2004**, *76*, 1754-1760.
- (56) Bush, M. F.; Hall, Z.; Giles, K.; Hoyes, J.; Robinson, C. V.; Ruotolo, B. T. *Anal. Chem.* **2010**, *82*, 9557-9565.
- (57) van Duijn, E.; Barendregt, A.; Synowsky, S.; Versluis, C.; Heck, A. J. R. *J. Am. Chem. Soc.* **2009**, *131*, 1452-1459.
- (58) Geels, R. B. J.; Calmat, S.; Heck, A. J. R.; van der Vies, S. M.; Heeren, R. M. A. *Rapid Commun. Mass Spectrom.* **2008**, *22*, 3633-3641.
- (59) Boeri Erba, E.; Ruotolo, B. T.; Barsky, D.; Robinson, C. V. *Anal. Chem.* **2010**, *82*, 9702-9710.
- (60) van Eldijk, M. B.; van Leeuwen, I.; Mikhailov, V. A.; Neijenhuis, L.; Harhangi, H. R.; van Hest, J. C. M.; Jetten, M. S. M.; den Camp, H. J. M. O.; Robinson, C. V.; Mecnovic, J. *Chem. Commun.* **2013**, *49*, 7770-7772.
- (61) Wanasundara, S. N.; Thachuk, M. *J. Phys. Chem. A* **2009**, *113*, 3814-3821.
- (62) Beardsley, R. L.; Jones, C. M.; Galhena, A. S.; Wysocki, V. H. *Anal. Chem.* **2009**, *81*, 1347-1356.
- (63) Han, L.; Ruotolo, B. T. *Anal. Chem.* **2015**, *87*, 6808-6813.
- (64) Griffin, L. L.; McAdoo, D. J. *J. Am. Soc. Mass Spectrom.* **1993**, *4*, 11-15.
- (65) Laskin, J.; Denisov, E.; Futrell, J. J. *J. Am. Chem. Soc.* **2000**, *122*, 9703-9714.
- (66) Fujii, N.; Mizuno, M.; Mizutani, Y. *J. Phys. Chem. B* **2011**, *115*, 13057-13064.
- (67) Helbing, J.; Devereux, M.; Nienhaus, K.; Nienhaus, G. U.; Hamm, P.; Meuwly, M. *J. Phys. Chem. A* **2012**, *116*, 2620-2628.
- (68) Martinez, L.; Figueira, A. C. M.; Webb, P.; Polikarpov, I.; Skaf, M. S. *J. Phys. Chem. Lett.* **2011**, *2*, 2073-2078.
- (69) Min, Z.; Politis, A.; Davies, R. B.; Liko, I.; Kuan-Jung, W.; Stewart, A. G.; Stock, D.; Robinson, C. V. *Nature Chem.* **2014**, *6*, 208-215.
- (70) Hunte, C.; Richers, S. *Curr. Opin. Struct. Biol.* **2008**, *18*, 406-411.

Authors are required to submit a graphic entry for the Table of Contents (TOC) that, in conjunction with the manuscript title, should give the reader a representative idea of one of the following: A key structure, reaction, equation, concept, or theorem, etc., that is discussed in the manuscript. Consult the journal's Instructions for Authors for TOC graphic specifications.

Insert Table of Contents artwork here

